Available online at sjuoz.uoz.edu.krd

journals.uoz.edu.krd

Science Journal of University of Zakho

Vol. 12, No.2, pp.227–236April-June, 2024

p-ISSN: 2663-628X
e-ISSN: 2663-6298

THE EFFECT OF FEATURE EXTRACTION ON COVID-19 CLASSIFICATION

Rebin Abdulkareem Hamaamin1, Shakhawan Hares Wady 2, Ali Wahab Kareem Sangawi 3
1Computer Science , College of Sciences, Charmo University, Chamchamal, Sulaimani, KRG, Iraq
Email: - rebin.abdulkarim@charmouniversity.org
2 Business Administration, College of Business, Charmo University, Chamchamal, Sulaimani, KRG, Iraq
Email: - shakhawan.hares@charmouniversity.org
3 General Science, College of Education, Charmo University, Chamchamal, Sulaimani, KRG, Iraq
Email: - ali.kareem@charmouniversity.org

Received: 15 Sep., 2023/ Accepted: 13 Mar., 2024 / Published: 3 June., 2024. https://doi.org/10.25271/sjuoz.2024.12.2.1204

ABSTRACT:

X-ray imaging stands as a prominent technique for diagnosing COVID-19, and it also serves as a crucial tool in the medical field for the analysis of various diseases. Numerous approaches are available to facilitate this analysis. Among these techniques, one involves the utilization of a Feature Extractor, which effectively captures pertinent characteristics from X-ray images. In a recent study, a comprehensive examination was conducted using 25 distinct feature extractors on X-ray images specific to COVID-19 cases. These images were categorized into two classes: COVID-19-positive and non-COVID-19. To enable a thorough evaluation, a sequence of machine learning classifiers was employed on these categorized images. The outcomes derived from this experimentation gauged the magnitude of impact that each individual feature exerted on COVID-19-related imagery. This assessment aimed to determine the efficacy levels of various feature extractors in terms of detection capability. Consequently, a distinction emerged between the more effective and less effective feature extractors, shedding light on their varying degrees of contribution to the detection process. Moreover, the comparative performance of different classifiers became evident, revealing the classifiers that exhibited superior performance when measured against their counterparts.

KEYWORDS: - Feature extraction, Machine learning, Effect of feature, X-Ray, Covid-19.

1. INTRODUCTION

The COVID-19 virus has a significant impact on individuals around the globe. The early diagnosis of this infectious disease is critical to prevent its global and local spread. Generally, scientists have tested numerous ways and methods to detect people and analyze the virus. Interestingly, one of the methods used for COVID-19 diagnosis is X-Rays that recognize whether the person is infected or not. Moreover, the researchers attempted to use methods and technologies that yielded quicker and more accurate results [1][2]. A series of feature extractors can be used to extract features from an image. A texture feature is one kind of feature. The texture is an important low-level feature in images, it can be used to characterize the contents of an image or a region. In addition to color features, color features alone cannot identify the image because distinct images can have similar histograms [3].

The essential factor here is to identify the relevant features and then choose the suitable classification method for these features. Once a set of features can be extracted from the images, it sends those features to machine learning for Classification. Classification is the process of categorizing a set of data into classes. It can be done on both structured and unstructured data. Determining the class of incoming data points is the first step in the procedure. The classes are also known as the target, label, or categories. Several machine learning classifiers are used to called Monogenic Binary Coding (MBC) [9]. Cigdem Turan and Kin-Man Lam in [10], some feature extractors were used in facial-expression recognition. All the features used are local descriptors. Seyyid Ahmed Medj in [11], states that a set of feature extractors has been developed to extract parts from images for both binary and multiclass. According to Samy Bakheet and Ayoub Al-Hamadi In [12] work has been done on the GLCM feature extractor to detect and diagnose COVID-19 classify data, such as Support Vector Machine (SVM), k-nearest neighbors (KNN), Ensemble, Decision Tree (DT), and Naïve Bayes (NB) [4].

To review the previous studies, the first part of the research discusses the effect of feature extractors on images. The second part highlights the research study on the diagnosis of COVID-19, which include [5] classification of histopathology images and identification of malignant areas using each feature extractor Gray-Level Co-Occurrence Matrix (GLCM), Local Binary Pattern (LBP), Local Binary Gray Level Co-occurrence Matrix (LBGLCM), gray-level run-length matrix (GLRLM) and Segmentation-based Fractal Texture Analysis (SFTA), Using SVM, KNN, Linear Discriminant Analysis (LDA) and Boosted Tree classifiers. The feature extractor is GLCM, GLRM, LBP, CLBP, and LTP and has been tested on the following diseases Brain, Breast, Colon, Skin, and Thyroid [6]. Also, in [7], A technique has been developed by combining both HOG and LBP feature extractors to identify plant leaves by SVM classifier. Taha J. Alhindi et al. in [8] state that work has been done on medical imaging using LBP, HOG, and a pre-trained deep network for histopathology images. For this purpose, support vector machines, decision trees, and artificial neural networks were used to identify and classify images through the obtained features. Another texture feature used to detect breast cancer in women is patients based on X-ray images, with it, the latent-dynamic conditional random fields (LDCRFs) classifier. Also, in [13], feature extractors extract features from images. in [14], Violent event has been worked on with two feature extractors for detecting a violent event.

The final section of this research discusses some papers that have worked on COVID-19 in general to diagnose the disease. Author in [15] proposed a new testing methodology to determine

* Corresponding author

whether a patient has been infected by the COVID-19 virus using the SDD300 model. The in-depth feature plus SVM-based procedure was proposed in [16] for identifying coronavirus-infected patients by applying CXR images. SVM was utilized for classification rather than DL-based classifiers, which require an extensive database for training and validation. A. Helwan et al. in [17] introduced a transfer learning approach to diagnose patients who tested positive for COVID-19 and distinguish them from healthy patients using ResNet-18, ResNet-50, and DenseNet-201. For this purpose, 2617 chest CT images of non-COVID-19 and COVID-19 have been experimented with.

M. Alruwaili et al. in [18] proposed an improved Inception-ResNetV2 DL model for accurately diagnosing chest CXR images. A Grad-CAM technique was also computed to improve the visibility of infected lung parts in CXR scans. D. Ji et al. in [19] presented a COVID-19 detection approach based on image modal feature fusion. Small-sample enhancement preprocessing, including spinning, translation, and randomized transformation, was initially conducted using this methodology. Five classic pertaining models, including VGG19, ResNet152, Xception, DenseNet201, and InceptionResnetV2, were used to extract CXR images' features. Pramod Gaur et al. in [20] presented an innovative methodology for preprocessing CT images and identifying COVID-19 positive and negative. The suggested approach used the principle of empiric wavelet transformation for preprocessing, with the optimal elements of the image's red, green, and blue channels being learned on the presented approach. Deep and transfer learning procedures as recommended by [21] to differentiate COVID-19 cases by assessing CXR images.

This paper uses a series of feature extractors to extract features from X-ray images of COVID-19. All the parts are sent to different classifiers. Then they are measured by several metrics to see which feature has higher results and has less impact on COVID-19. The following is the flow of this paper. Section 2 highlights the methods used to extract features on the COVID-19 image and the classifiers used with the evaluation metrics. In section 3, All results are presented with different classifiers for each classifier, a set of metrics used to measure the data. The conclusion is described in the last section.

Material and Methodology

The process by which features are extracted from images in this research is visually outlined in Figure (1). This diagram succinctly portrays the procedural steps and components utilized to carry out the feature extraction from the images under investigation. It serves as a graphical representation of the methodology, aiding in conveying a clear understanding of the sequential and conceptual aspects of how image features are harnessed for analysis within the context of this study. In this system, a standard database is used to test several feature extractors to distinguish between COVID-19 and non-COVID-19 by several classifiers to take the effect of each feature extractor to see which good results are measured by several metrics.

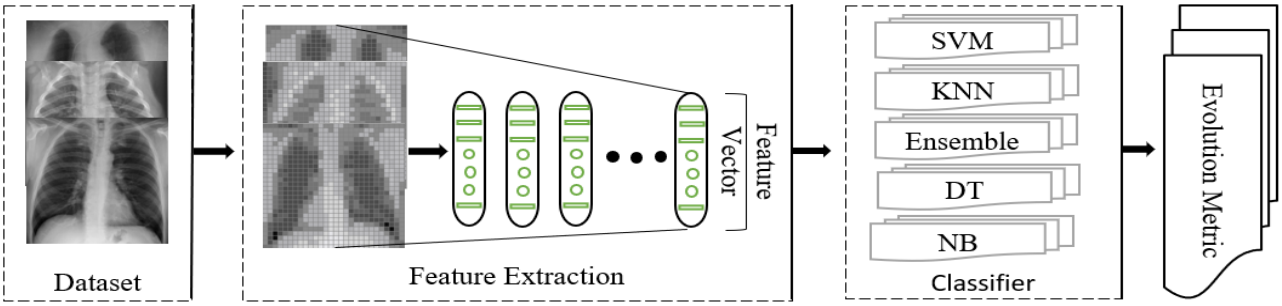

Figure 1: System overview.

1.1 Dataset

The COVID-19 radiographic database, a publicly available database, is used in this paper. The database consists of 21165 CXR images, of which 10,192 belong to normal, 3616 correspond to COVID-19 positive, and 6012 belong to lung opacity (non-COVID lung infection), and 1345 are labeled as viral pneumonia cases. The data for this paper includes 7232 CXR images, 3616 of which with a positive COVID-19 diagnosis and 3616 negative cases randomly selected to create the balanced database. All images in the database have been preprocessed before being featured as follows: Figure (2) visually represents the sequential process involved in the manipulation of images. The initial step involves converting the images into grayscale, resulting in representations composed solely of varying shades of gray. In the subsequent step, all images are uniformly resized to dimensions of 512 x 512 pixels. Finally, the region of interest (ROI) is meticulously extracted from each image. This ROI encapsulates specific, critical features relevant to the analysis. The figure provides a graphical overview of these operations, effectively illustrating the transformation process, from grayscale conversion and resizing to the selective extraction of the region of interest.

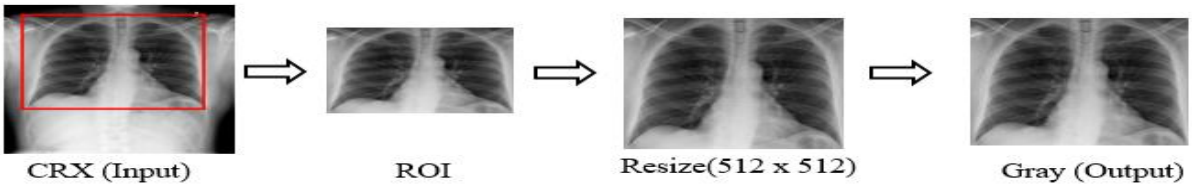

Figure 2: Preprocessing overall framework

1.2. Feature extraction

Feature extraction is the technique of extracting numbers from data using unique processing that allows you to operate on the original data without destroying it. It produces better results than working with raw data, and it makes them faster. In this study, a total of twenty-five distinct feature extractors were employed to extract features from the data. Each of these extractors possessed a unique set of features, employing varied techniques, as comprehensively outlined in Table (1).

Table 1: The list of feature extractors.

N	Feature Extractors	No. Features
1	Gray Level Run Length Matrix (GLRLM)	8
2	Gray Level Co-occurrence Matrix (GLCM)	22
3	Weber Local Descriptor (WLD)	32
4	Local Gradient Increasing Pattern (LGIP)	37
5	Gabor Wavelet (GW)	48
6	Local Directional Pattern (LDiP)	56
7	Local Directional Number Pattern (LDNP)	56
8	Local Directional Texture Pattern (LDTP)	72
9	Wavelet Transform (WT)	72
10	Histogram of Oriented Gradients (HOG)	81
11	Pyramid of Histogram of Oriented Gradients (PHOG)	168
12	Local Monotonic Pattern (LMP)	256
13	Local Phase Quantization (LPQ)	256
14	Local Transitional Pattern (LTrP)	256
15	Median Binary Pattern (MBP)	256
16	Gradient Directional Pattern (GDP)	256
17	Local Arc Pattern (LAP)	272
18	Local Frequency Descriptor (LFD)	512
19	Median Ternary Pattern (MTP)	512
20	Local Ternary Pattern (LTeP)	512
21	Gradient Local Ternary Pattern (GLTP)	512
22	Median Robust Extended Local Binary Pattern (MRELBP)	800
23	Binary Pattern of Phase Congruency (BPPC)	1062
24	Improved Weber Binary Coding (IWBC)	2048
25	Monogenic Binary Coding (MBC)	3072

1.3. Classification and Evaluation

After the features are extracted from the images, they are sent to the machine learning classifier. Basically, classifiers are algorithms that automatically sort or categorize data into one or more classes known as ‘Classification’. Classes are referred to as targets, labels, and categories. This research used a set of classifiers to separate the data into two types: COVID-19 and non-COVID-19. The classifiers used in this research are the KNN: which is a supervised machine learning algorithm method that can be used to solve both classification and regression problems and is simple to implement [22]. The second classifier is Ensemble, a method for creating a variety of base classifiers [23]. The third classifier is DT: This model works by parsing our data into a DT. The fourth classifier is NB: a set of straightforward "probabilistic classifiers" based on Bayes' theorem and strong (naive) independence [22]. Furthermore, the last classifier SVM, a supervised machine learning technique that can be used to solve classification and regression problems. In SVM used, different kernels for classifying data, the SVM linear kernel (SVML), SVM Radial Basis Function kernel (SVMRBF), and SVM polynomial kernel (SVMP) [24][25]. All three types of

kernels were tested in the research. The final part of the study is to tether data with several different metrics to see how each feature receptor affects the image of COVID-19 [26].

2. EXPERIMENTAL RESULTS AND DISCUSSIONS

Numerous texture feature descriptors as presented in Table (1), were generated for assessing the CXR images of COVID-19, which is either positive or negative, and the result were given as second opinion to the clinicians to make exact decisions. Besides, to classify the CXR images, five well-known ML classifiers were utilized, namely, SVM (linear, RBF, and polynomial), KNN, Ensemble, DT, and NB classifiers. From the experiments performed on COVID-19 radiography dataset, the analysis of each descriptor was estimated in terms of a series of indicators (F-Score, Matthew's correlation coefficient (MCC) specificity, precision, sensitivity, and Accuracy) with Ensemble (Table 2), KNN (Table 3), NB (Table 4), DT (Table 5), SVML (Table 6), SVMRBF (Table 7), and SVMP (Table 8) classifiers respectively.

As depicted in the initial experiment detailed in Table (2), the MRELBP feature descriptor emerged as the frontrunner. It exhibited the highest accuracy rate of 95.09% across all metrics, in tandem with the Ensemble classifier. In contrast, the classification accuracy stemming from the GLRLM method lagged behind, registering a comparatively lower score of 78.15%.

Table 2: All the feature extractors used in the Ensemble Classifier

		Measurement Metrics					
N	Feature Extractor	F- Score	MCC	Specificity	Precision	Sensitivity	Accuracy
1	WT	43.35	73.53	87.25	86.27	87.13	86.76
2	GLCM	42.11	68.96	85.98	82.95	85.54	84.46
3	GLRLM	39.07	56.33	78.30	78.01	78.25	78.15
4	HOG	45.83	83.31	91.62	91.69	91.64	91.65
5	GW	42.08	69.33	87.43	81.78	86.68	84.61
6	BPPC	46.47	85.85	92.78	93.06	92.81	92.92
7	GDP	45.07	80.36	90.51	89.83	90.46	90.17
8	GLTP	45.43	81.86	91.69	90.15	91.56	90.92
9	LAP	45.08	80.42	90.69	89.70	90.62	90.19
10	LDNP	44.47	78.12	90.03	88.06	89.84	89.05
11	LDTP	42.12	68.66	84.90	83.75	84.73	84.32
12	LFD	44.63	78.52	89.20	89.32	89.21	89.26
13	LMP	46.04	84.17	92.10	92.06	92.11	92.08
14	LPQ	46.23	84.94	92.61	92.32	92.60	92.47
15	LTrP	45.07	80.20	89.67	90.53	89.76	90.10
16	LDiP	44.60	78.47	89.59	88.87	89.52	89.23
17	WLD	40.56	62.39	81.60	80.77	81.47	81.19
18	MBC	45.91	83.76	92.60	91.13	92.50	91.87
19	IWBC	46.38	85.53	92.88	92.64	92.87	92.76
20	PHOG	45.47	81.94	91.23	90.69	91.20	90.96
21	LGIP	45.31	81.25	90.59	90.65	90.61	90.62
22	MRELBP	47.54	90.19	95.17	95.01	95.17	95.09
23	MBP	44.89	79.62	90.14	89.47	90.08	89.81
24	MTP	40.92	64.45	84.15	80.24	83.51	82.19
25	LTeP	44.68	78.90	90.29	88.59	90.13	89.44

Upon the utilization of the KNN classifier, distinct categories of features exhibited disparate responses in terms of their projected performance. The findings, as elucidated in Table (3), indicate that the MRELBP method showcased notable efficacy, achieving an accuracy rate of 91.59% in the classification of chest X-ray (CXR) images when juxtaposed with the array of alternative techniques implemented.

Table 3: All the feature extractors used in the KNN Classifier

		Measurement Metrics					
N	Feature extractor	F- score	MCC	Specificity	Precision	Sensitivity	Accuracy
1	WT	42.86	71.21	84.70	86.49	84.98	85.59
2	GLCM	42.02	68.02	83.79	84.22	83.86	84.00
3	GLRLM	37.93	50.66	73.02	77.58	74.20	75.30
4	HOG	44.98	79.56	87.58	91.89	88.10	89.74
5	GW	41.21	64.53	81.34	83.15	81.69	82.25
6	BPPC	45.65	82.44	90.07	92.34	90.30	91.20

7	GDP	44.25	76.56	86.04	90.43	86.64	88.24
8	GLTP	42.86	70.62	81.66	88.77	82.88	85.21
9	LAP	43.62	74.00	84.83	89.09	85.47	86.96
10	LDNP	42.69	70.07	82.27	87.69	83.19	84.98
11	LDTP	39.80	59.44	80.36	79.06	80.13	79.71
12	LFD	42.99	71.18	82.30	88.73	83.39	85.51
13	LMP	44.53	77.45	84.26	92.89	85.52	88.58
14	LPQ	45.19	80.41	87.79	92.53	88.34	90.16
15	LTrP	43.25	71.95	80.17	91.31	82.17	85.74
16	LDiP	43.06	71.61	83.04	88.44	83.93	85.74
17	WLD	39.14	55.58	75.35	80.15	76.51	77.75
18	MBC	45.45	81.48	88.56	92.84	89.04	90.70
19	IWBC	44.71	78.16	83.24	94.41	84.94	88.82
20	PHOG	43.80	74.40	82.82	91.30	84.17	87.06
21	LGIP	43.91	74.92	83.61	91.09	84.76	87.35
22	MRELBP	45.86	83.23	90.08	93.10	90.39	91.59
23	MBP	43.18	71.76	81.09	90.36	82.70	85.73
24	MTP	38.63	54.65	77.61	77.04	77.48	77.32
25	LTeP	40.79	62.23	78.26	83.86	79.43	81.06

Another classifier used in the research is NB. It is a probabilistic machine learning algorithm based on the Bayes theorem. This classifier has a problem that when a feature that is output contains a zero result, this classifier does not output a result, and the result is non. As depicted in Table (4), the feature structures encompassing MRELBP, MBP, MTP, and LTep have yielded non-results, reflecting zero outcomes in their respective feature sets. In contrast, among the other feature extractors explored in this study, the highest achievement was observed with the PHOG feature extractor, achieving a noteworthy accuracy score of 80.80% in the accuracy metric specifically for COVID-19 detection. Notably, when these results are juxtaposed with the preceding ones, it becomes apparent that they fall short in comparison to the outcomes generated by the diverse classifier implementations.

Table 4: All the feature extractors used in the NB Classifier

		Measurement Metrics					
N	Feature extractor	F- score	MCC	Specificity	Precision	Sensitivity	Accuracy
1	WT	37.75	51.62	77.03	74.56	76.47	75.80
2	GLCM	37.70	52.47	79.32	73.04	77.93	76.18
3	GLRLM	35.45	35.75	55.08	79.57	63.92	67.32
4	HOG	39.56	56.26	72.43	83.47	75.19	77.95
5	GW	33.96	45.92	85.33	58.95	80.09	72.14
6	BPPC	39.68	55.81	67.84	86.93	73.01	77.39
7	GDP	38.63	52.95	72.57	80.21	74.52	76.39
8	GLTP	35.15	41.62	72.45	69.14	71.52	70.80
9	LAP	39.04	52.73	65.35	86.21	71.34	75.78
10	LDNP	38.00	49.51	68.67	80.48	71.98	74.58
11	LDTP	25.65	36.51	93.32	36.79	84.66	65.06
12	LFD	37.81	47.01	61.80	84.02	68.75	72.91
13	LMP	39.17	54.32	70.36	83.47	73.81	76.92
14	LPQ	40.28	59.28	73.76	85.13	76.45	79.45
15	LTrP	37.08	44.13	61.85	81.40	68.11	71.63
16	LDiP	37.30	46.07	65.64	79.94	69.94	72.79
17	WLD	33.20	42.41	82.90	58.19	77.29	70.55
18	MBC	39.77	56.76	71.00	85.19	74.60	78.09
19	IWBC	39.36	55.05	70.50	84.04	74.02	77.27
20	PHOG	40.87	61.94	75.62	85.98	77.92	80.80
21	LGIP	37.57	46.77	64.74	81.37	69.78	73.06
22	MRELBP	-	-	-	-	-	-
23	MBP	-	-	-	-	-	-

24	MTP	-	-	-	-	-	-
25	LTeP	-	-	-	-	-	-

DT is another classifier implemented in this paper. This classifier works as a tree on the nodes and then extends the branches down. The only reason these classifiers were used in these feature extractions was to examine how they performed compared to other classifiers. The results obtained from this classifier are weaker than the KNN and ensemble classifiers, presented in Table (5), parallel to the assortment of classifiers, the optimal feature extractor remains MRELBP. Remarkably, among the alternative feature extraction approaches, Access achieves the peak outcome of 85.50%, standing out as the most elevated result among the other feature extractors.

Table 5: All the feature extractors used in the DT Classifier

		Measurement Metrics					
N	Feature extractor	F- score	MCC	Specificity	Precision	Sensitivity	Accuracy
1	WT	40.01	59.85	79.39	80.44	79.61	79.92
2	GLCM	40.11	60.38	80.01	80.35	80.09	80.18
3	GLRLM	36.35	44.99	71.78	73.20	72.20	72.49
4	HOG	41.43	65.45	81.89	83.54	82.20	82.72
5	GW	38.32	53.19	76.38	76.79	76.50	76.58
6	BPPC	41.62	66.49	83.20	83.28	83.21	83.24
7	GDP	41.12	64.05	80.72	83.28	81.22	82.00
8	GLTP	41.00	63.79	81.31	82.45	81.54	81.88
9	LAP	40.65	62.48	80.91	81.55	81.05	81.23
10	LDNP	40.03	60.08	79.92	80.15	79.96	80.03
11	LDTP	38.33	53.54	77.18	76.32	77.02	76.75
12	LFD	40.30	61.01	79.99	81.01	80.20	80.50
13	LMP	41.65	66.55	83.13	83.40	83.20	83.26
14	LPQ	41.91	67.41	82.99	84.40	83.24	83.69
15	LTrP	40.44	61.55	80.26	81.27	80.48	80.77
16	LDiP	41.07	63.88	80.76	83.08	81.23	81.92
17	WLD	36.50	45.59	72.05	73.53	72.47	72.79
18	MBC	41.12	64.66	82.85	81.80	82.67	82.32
19	IWBC	41.61	66.20	82.38	83.80	82.64	83.09
20	PHOG	40.16	60.28	79.24	81.02	79.61	80.13
21	LGIP	41.42	65.80	83.26	82.53	83.15	82.90
22	MRELBP	42.74	71.03	85.74	85.26	85.69	85.50
23	MBP	40.32	61.19	80.32	80.86	80.43	80.59
24	MTP	37.64	50.21	74.41	75.75	74.80	75.08
25	LTeP	39.00	55.90	77.73	78.15	77.85	77.94

Tables (6 - 8) comprehensively present the performance outcomes of all SVM models. Drawing insights from the research findings across the three distinct kernels, a consistent pattern emerges: the features extracted through the utilization of MRELBP techniques consistently outshine alternative scenarios. This phenomenon is evident when employing the SVML, SVMRBF, and SVMP classifiers, where the corresponding accuracy rates for MRELBP features stand at 85.50%, 95.10%, and an impressive 95.87%, respectively. This consistency in the detection and classification. superiority of MRELBP-derived features across diverse SVM kernels underscores the robustness and effectiveness of this feature extraction approach. The exceptional accuracy rates obtained with SVMP highlight its particular aptitude in capturing the relevant patterns present in the data, contributing to accurate classification of COVID-19 images. Consequently, these findings emphasize the potential of MRELBP-based features in enhancing the performance and accuracy of machine learning models for disease

Table 6: All the feature extractors used in the SVML Classifier

		Measurement Metrics					
N	Feature extractor	F- score	MCC	Specificity	Precision	Sensitivity	Accuracy
1	WT	39.63	58.41	78.92	79.47	79.05	79.20
2	GLCM	38.14	54.82	81.62	72.99	79.90	77.30
3	GLRLM	39.35	54.45	67.91	85.66	72.77	76.78
4	HOG	44.50	77.75	87.66	90.06	87.96	88.86
5	GW	40.91	67.14	90.73	75.63	89.10	83.18
6	BPPC	46.23	84.91	92.37	92.53	92.39	92.45
7	GDP	43.86	75.66	88.67	86.97	88.48	87.82
8	GLTP	44.38	77.97	90.79	87.12	90.44	88.96
9	LAP	43.42	73.64	86.71	86.93	86.74	86.82
10	LDNP	41.95	67.91	84.27	83.62	84.17	83.95
11	LDTP	40.82	65.40	87.44	77.63	86.08	82.54
12	LFD	43.53	73.84	85.67	88.13	86.02	86.90
13	LMP	44.90	79.45	88.99	90.44	89.16	89.72
14	LPQ	45.85	83.35	91.42	91.91	91.49	91.67
15	LTrP	43.12	72.49	86.29	86.18	86.29	86.24
16	LDiP	43.97	75.97	88.37	87.59	88.29	87.98
17	WLD	38.50	56.30	82.56	73.49	80.85	78.02
18	MBC	46.23	85.04	93.28	91.74	93.19	92.51
19	IWBC	45.44	81.66	90.18	91.45	90.33	90.82
20	PHOG	44.68	78.50	88.13	90.35	88.39	89.24
21	LGIP	42.74	71.39	87.05	84.29	86.71	85.67
22	MRELBP	46.48	85.76	91.60	94.12	91.82	92.86
23	MBP	43.49	74.36	88.66	85.66	88.33	87.16
24	MTP	40.32	63.84	87.32	76.11	85.72	81.72
25	LTeP	42.34	70.57	88.56	81.84	87.74	85.20

Table 7: All the feature extractors used in the SVMRBF Classifier

		Measurement Metrics					
N	Feature extractor	F- score	MCC	Specificity	Precision	Sensitivity	Accuracy
1	WT	44.33	77.67	90.21	87.41	89.95	88.81
2	GLCM	42.88	72.33	88.64	83.58	88.05	86.11
3	GLRLM	39.37	58.28	80.86	77.36	80.19	79.11
4	HOG	46.62	86.53	93.57	92.96	93.53	93.26
5	GW	42.24	71.56	91.92	79.03	90.74	85.48
6	BPPC	47.29	89.15	94.34	94.80	94.37	94.57
7	GDP	45.86	83.47	91.89	91.56	91.87	91.73
8	GLTP	44.98	80.42	92.32	88.01	91.98	90.17
9	LAP	45.60	82.52	91.96	90.54	91.86	91.25
10	LDNP	45.42	81.69	90.75	90.93	90.77	90.84
11	LDTP	40.99	62.31	75.19	86.69	77.77	80.94
12	LFD	45.37	81.48	90.72	90.75	90.74	90.73
13	LMP	46.93	87.80	94.63	93.15	94.56	93.89
14	LPQ	47.23	88.93	94.54	94.38	94.54	94.46
15	LTrP	45.57	82.25	91.04	91.20	91.06	91.12
16	LDiP	45.09	80.63	91.45	89.14	91.26	90.30
17	WLD	41.34	66.36	85.75	80.50	85.00	83.13
18	MBC	46.54	86.30	93.94	92.34	93.85	93.14
19	IWBC	46.68	86.67	92.79	93.86	92.88	93.33
20	PHOG	46.25	85.10	93.07	92.02	93.00	92.54
21	LGIP	46.03	84.22	92.56	91.65	92.50	92.10
22	MRELBP	47.53	90.21	95.84	94.36	95.78	95.10

23	MBP	45.96	83.92	92.48	91.44	92.40	91.96
24	MTP	38.91	52.33	65.91	85.41	71.49	75.66
25	LTeP	42.36	68.31	79.35	88.66	81.13	84.00

Table 8: All the feature extractors used in the SVMP Classifier

		easurement Metrics					
N	Feature extractor	F- score	MCC	Specificity	Precision	Sensitivity	Accuracy
1	WT	43.71	75.07	88.33	86.72	88.14	87.52
2	GLCM	43.17	73.46	89.23	84.12	88.66	86.67
3	GLRLM	31.41	16.26	32.43	80.30	51.60	56.37
4	HOG	46.72	86.82	92.85	93.96	92.93	93.40
5	GW	44.57	78.26	88.98	89.27	89.02	89.12
6	BPPC	47.21	88.83	94.19	94.63	94.22	94.41
7	GDP	45.75	82.87	90.59	92.25	90.76	91.42
8	GLTP	45.48	81.89	90.72	91.16	90.77	90.94
9	LAP	45.60	82.21	89.86	92.31	90.11	91.09
10	LDNP	45.93	83.56	90.55	92.97	90.79	91.76
11	LDTP	39.26	44.33	57.28	86.47	71.91	71.87
12	LFD	45.44	81.62	89.90	91.70	90.08	90.80
13	LMP	47.11	88.36	93.62	94.73	93.70	94.18
14	LPQ	47.52	90.04	94.40	95.63	94.47	95.01
15	LTrP	45.67	82.50	90.11	92.37	90.34	91.24
16	LDiP	45.85	83.21	90.39	92.79	90.62	91.59
17	WLD	43.17	72.41	85.10	87.28	85.44	86.19
18	MBC	46.83	87.30	93.58	93.71	93.60	93.64
19	IWBC	46.89	87.47	92.82	94.62	92.96	93.72
20	PHOG	46.38	85.46	92.16	93.29	92.25	92.72
21	LGIP	46.73	86.83	92.64	94.18	92.76	93.41
22	MRELBP	47.94	91.75	95.44	96.31	95.48	95.87
23	MBP	46.03	84.00	91.15	92.84	91.30	91.99
24	MTP	34.62	11.61	26.61	81.15	60.37	53.88
25	LTeP	44.49	77.92	88.80	89.11	88.85	88.96

Upon extensive evaluation of various feature extractors with diverse classifiers, noteworthy findings have emerged. Notably, the most effective feature extractor across all classifiers, with the exception of the NB classifier, is determined to be MRELBP. However, it is worth highlighting that MRELBP yields no results within the NB classifier due to its lack of features, resulting in a count of zero. Intriguingly, within the context of the NB classifier, the optimal feature extractor is identified as PHOG. These outcomes, outlined in Figure 2, distinctly outline the superiority of specific feature extractors within distinct classifier contexts, thus contributing valuable insights to the overall research findings.

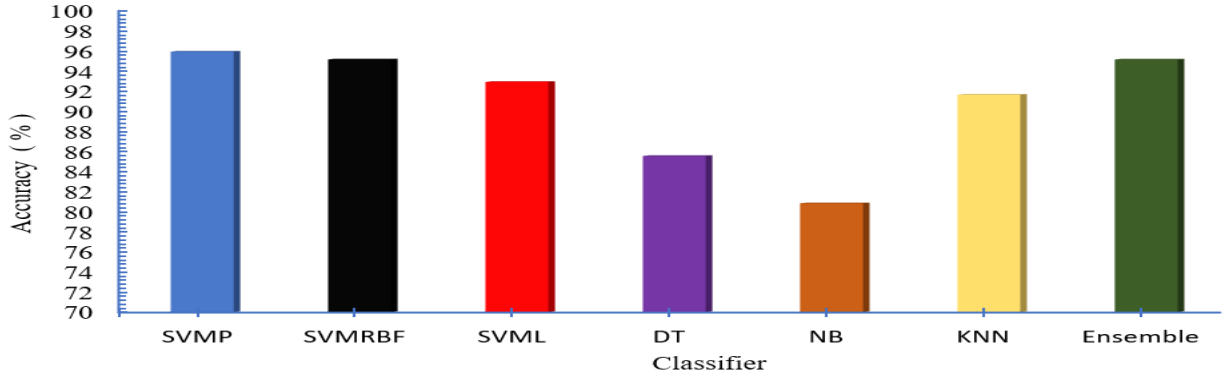

Figure 3: effect of feature extraction on Covid-19 images in different classifier

In our analysis of various works, it has become evident that the features employed in this study surpass several other functions, particularly those highlighted in Table (9). However, the real potential lies in the synergy achieved through combining these features, leading to improved results. This underscores the importance of a holistic approach in leveraging the strengths of individual features for a more comprehensive and effective outcome.

Table 9: Comparison of proposed classification accuracy with existing state-of-the-art techniques

Previous study	Methods/ classifier	Accuracy (%)
A. I. Khan et al[27]	(CNN) CoroNet	89.60
A. Zargari Khuzani et al[28]	ResNet-18	92.49
L. Wang et al[1]	COVID-Net	93.30
M. Owais et al[29]	Ensemble-Net	94.72
F. Saiz and I. Barandiaran[15]	SDD300	94.92
F. H. Ahmad and S. H. Wady[30]	SVM (CT+GWT+LGIP)	96.18
R. A. Hamaamin et al[31]	HOG +LPQ	97.15
R. A. Hamaamin et al[32]	Resnet 50	98.05
Proposed	MRELBP	95.87

CONCLUSION

Due to the global prevalence of the COVID-19 pandemic, a multitude of researchers have been diligently striving to devise an intelligent approach for the swift identification of the disease. One prominent technique within this realm involves the utilization of feature extractors to distill pertinent information from images. In this pursuit, a particular study undertook the deployment of a series of feature extractors to scrutinize COVID-19 images, aiming to discern the optimal feature extraction methodology.

Through a meticulous evaluation of diverse feature extractors, this research endeavors to unearth the most efficacious one. Among the twenty-five feature extractors subjected to assessment, certain features emerged with exceptional efficacy in delineating the disease. Notably, the investigation pinpointed "MRELBP" as the preeminent feature extractor, showcasing a remarkable accuracy rate of 95.87% when employed in conjunction with the SVMP classifier. It is worth mentioning that this study exhibited a comprehensive approach, encompassing an array of classifiers to culminate in its findings. Moreover, a multifaceted set of metrics was employed to gauge the performance of each featured extractor.

The primary issue with the study lies in the time-consuming nature of obtaining results for certain features. Furthermore, some features are sourced from machine learning missions that were not undertaken

REFERENCES

Wei Wang, Yutao Li, Ji Li, Peng Zhang, Xin Wang, "Detecting COVID-19 in Chest X-Ray Images via MCFF-Net", Computational Intelligence and Neuroscience, vol. 2021, Article ID 3604900, 8 pages, 2021. https://doi.org/10.1155/2021/3604900.

Ebrahim Mohammed Senan, Ali Alzahrani, Mohammed Y. Alzahrani, Nizar Alsharif, Theyazn H. H. Aldhyani, "Automated Diagnosis of Chest X-Ray for Early Detection of COVID-19 Disease", Computational and Mathematical Methods in Medicine, vol. 2021, Article ID 6919483, 10 pages, 2021. https://doi.org/10.1155/2021/6919483.

J. Lian, M. Zhang, N. Jiang, W. Bi, and X. Dong, “Feature Extraction of Kidney Tissue Image Based on Ultrasound Image Segmentation,” J. Healthc. Eng., vol. 2021, 2021, doi: 10.1155/2021/9915697.

Nugrahaeni, Ratna Astuti and Kusprasapta Mutijarsa. “Comparative analysis of machine learning KNN, SVM, and random forests algorithm for facial expression classification.” 2016 International Seminar on Application for Technology of Information and Communication (ISemantic) (2016): 163-168.

Ş. Öztürk and B. Akdemir, “ScienceDirect ScienceDirect ScienceDirect Application of Feature Extraction and Classification Methods for Histopathological Image using GLCM , Application of Feature Extraction and Classification Methods for and GLCM , Histopathological Image using a SFTA,” Procedia Comput. Sci., vol. 132, no. Iccids, pp. 40–46, 2018, doi: 10.1016/j.procs.2018.05.057.

Vani Kumari, S., Usha Rani, K. (2020). Analysis on Various Feature Extraction Methods for Medical Image Classification. In: Jyothi, S., Mamatha, D., Satapathy, S., Raju, K., Favorskaya, M. (eds) Advances in Computational and Bio-Engineering. CBE 2019. Learning and Analytics in Intelligent Systems, vol 16. Springer, Cham. https://doi.org/10.1007/978-3-030-46943-6_3.

Keivani, M., Mazloum, J., Sedaghatfar, E., Tavakoli, M.B. (2020). Automated analysis of leaf shape, texture, and color features for plant classification. Traitement du Signal, Vol. 37, No. 1, pp. 17-28. https://doi.org/10.18280/ts.370103.

T. J. Alhindi, S. Kalra, K. H. Ng, A. Afrin, and H. R. Tizhoosh, “Comparing LBP , HOG and Deep Features for Classification of Histopathology Images,” 2018 Int. Jt. Conf. Neural Networks, pp. 1–7, 2018, doi: 10.1109/IJCNN.2018.8489329.

E. Mohammadi, E. Fatemizadeh, H. Sheikhzadeh, and S. Khoubani, “A Textural Approach for Recognizing Architectural Distortion In Mammograms,” pp. 136–140, 2013.

C. Turan and K. Lam, “Histogram-based Local Descriptors for Facial Expression Recognition (FER): A comprehensive

Study," J. Vis. Commun. Image Represent., 2018, doi: 10.1016/j.jvcir.2018.05.024.

S. A. Medjahed, "A Comparative Study of Feature Extraction Methods in Images Classification," no. February, pp. 16–23, 2015, doi: 10.5815/ijigsp.2015.03.03.

S. Bakheet and A. Al-hamadi, "Automatic detection of COVID-19 using pruned GLCM-Based texture features and LDCRF classification," Comput. Biol. Med., vol. 137, no. August, p. 104781, 2021, doi: 10.1016/j.compbiomed.2021.104781.

Saipullah, K.M., Kim, DH. A robust texture feature extraction using the localized angular phase. Multimed Tools Appl 59, 717–747 (2012). https://doi.org/10.1007/s11042-011-0766-5.

M. Aradhya and D. S. Guru, "Violent Video Event Detection Based on Integrated LBP and GLCM Texture Features Revue d ' Intelligence Artificielle Violent Video Event Detection Based on Integrated LBP and GLCM Texture Features," no. May, 2020, doi: 10.18280/ria.340208.

F. Saiz and I. Barandiaran, "COVID-19 Detection in Chest X-ray Images using a Deep Learning Approach," Int. J. Interact. Multimed. Artif. Intell., vol. 6, no. 2, p. 4, 2020, doi: 10.9781/ijimai.2020.04.003.

A. K. Singh, A. Kumar, M. Mahmud, M. S. Kaiser, and A. Kishore, "COVID-19 Infection Detection from Chest X-Ray Images Using Hybrid Social Group Optimization and Support Vector Classifier," Cognit. Comput., no. 0123456789, 2021, doi: 10.1007/s12559-021-09848-3.

A. Helwan, M. K. S. Ma'Aitah, H. Hamdan, D. U. Ozsahin, and O. Tuncyurek, "Radiologists versus Deep Convolutional Neural Networks: A Comparative Study for Diagnosing COVID-19," Comput. Math. Methods Med., vol. 2021, 2021, doi: 10.1155/2021/5527271.

M. Alruwaili, A. Shehab, and S. Abd El-Ghany, "COVID-19 Diagnosis Using an Enhanced Inception-ResNetV2 Deep Learning Model in CXR Images," J. Healthc. Eng., vol. 2021, no. Dl, 2021, doi: 10.1155/2021/6658058.

D. Ji, Z. Zhang, Y. Zhao, and Q. Zhao, "Research on Classification of COVID-19 Chest X-Ray Image Modal Feature Fusion Based on Deep Learning," J. Healthc. Eng., vol. 2021, 2021, doi: 10.1155/2021/6799202.

P. Gaur, V. Malaviya, A. Gupta, G. Bhatia, R. B. Pachori, and D. Sharma, "COVID-19 disease identification from chest CT images using empirical wavelet transformation and transfer learning," Biomed. Signal Process. Control, vol. 71, no. PA, p. 103076, 2022, doi: 10.1016/j.bspc.2021.103076.

Talal S. Qaid, Hussein Mazaar, Mohammad Yahya H. Al-Shamri, Mohammed S. Alqahtani, Abeer A. Raweh, Wafaa Alakwaa, "Hybrid Deep-Learning and Machine-Learning Models for Predicting COVID-19", Computational Intelligence and Neuroscience, vol. 2021, Article ID 9996737, 11 pages, 2021. https://doi.org/10.1155/2021/9996737

Aljabri, Malak, Amal A. Alahmadi, Rami Mustafa A. Mohammad, Menna Aboulnour, Dorieh M. Alomari, and Sultan H. Almotiri. 2022. "Classification of Firewall Log Data Using Multiclass Machine Learning Models" Electronics 11, no. 12: 1851. https://doi.org/10.3390/electronics11121851.

Dietterich, T.G. (2000). Ensemble Methods in Machine Learning. In: Multiple Classifier Systems. MCS 2000. Lecture Notes in Computer Science, vol 1857. Springer, Berlin, Heidelberg. https://doi.org/10.1007/3-540-45014-9_1

S. A. Jafar Zaidi, I. Chatterjee, and S. Brahim Belhaouari, "COVID-19 Tweets Classification during Lockdown Period Using Machine Learning Classifiers," Appl. Comput. Intell. Soft Comput., vol. 2022, 2022, doi: 10.1155/2022/1209172.

J. Zeng et al., "Prediction of peak particle velocity caused by blasting through the combinations of boosted-chaid and svm models with various kernels," Appl. Sci., vol. 11, no. 8, 2021, doi: 10.3390/app11083705.

U. Özkaya, Ş. Öztürk, and M. Barstugan, "Coronavirus (COVID-19) Classification Using Deep Features Fusion and Ranking Technique," Stud. Big Data, vol. 78, pp. 281–295, 2020, doi: 10.1007/978-3-030-55258-9_17.

A. I. Khan, J. L. Shah, and M. M. Bhat, "CoroNet: A deep neural network for detection and diagnosis of COVID-19 from chest x-ray images," Comput. Methods Programs Biomed., vol. 196, p. 105581, 2020, doi: 10.1016/j.cmpb.2020.105581.

A. Zargari Khuzani, M. Heidari, and S. A. Shariati, "COVID-Classifier: an automated machine learning model to assist in the diagnosis of COVID-19 infection in chest X-ray images," Sci. Rep., vol. 11, no. 1, pp. 1–6, 2021, doi: 10.1038/s41598-021-88807-2.

M. Owais, H. S. Yoon, T. Mahmood, A. Haider, H. Sultan, and K. R. Park, "Light-weighted ensemble network with multilevel activation visualization for robust diagnosis of COVID19 pneumonia from large-scale chest radiographic database," Appl. Soft Comput., vol. 108, no. April, p. 107490, 2021, doi: 10.1016/j.asoc.2021.107490.

F. H. Ahmad and S. H. Wady, "COVID-19 Infection Detection from Chest X-Ray Images Using Feature Fusion and Machine Learning," Sci. J. Cihan Univ. – Sulaimaniya, vol. 5, no. 2, pp. 10–30, 2021.

R. A. Hamaamin, S. H. Wady, and A. W. Kareem, "Classification of COVID-19 on Chest X-Ray Images Through the Fusion of HOG and LPQ Feature Sets," vol. 4, no. 2, pp. 135–143, 2022, doi: 10.24271/psr.51.

Hamaamin, R. A., Wady, S. H., & Sangawi, A. W. K. (2022). COVID-19 Classification based on Neutrosophic Set Transfer Learning Approach. UHD Journal of Science and Technology, 6(2), 11–18. https://doi.org/10.21928/uhdjst.v6n2y2022.pp11-18.